

## Etching of nanopatterns in silicon using nanopantography

Lin Xu

*Department of Chemical and Biomolecular Engineering, Plasma Processing Laboratory, University of Houston, Houston, Texas 77204-4004, USA*

Azeem Nasrullah

*Department of Electrical and Computer Engineering, University of Houston, Houston, Texas 77204, USA*

Zhiying Chen and Manish Jain

*Department of Chemical and Biomolecular Engineering, Plasma Processing Laboratory, University of Houston, Houston, Texas 77204-4004, USA*

Paul Ruchhoeft

*Department of Electrical and Computer Engineering, University of Houston, Houston, Texas 77204, USA*

Demetre J. Economou<sup>a)</sup> and Vincent M. Donnelly<sup>b)</sup>

*Department of Chemical and Biomolecular Engineering, Plasma Processing Laboratory, University of Houston, Houston, Texas 77204-4004, USA*

(Received 23 September 2007; accepted 4 December 2007; published online 9 January 2008)

Nanopantography is a technique for parallel writing of nanopatterns over large areas. A broad ion beam impinges on a substrate containing many microfabricated electrostatic lenses that focus ions to spots at the substrate surface. Here, etching of nanopatterns is demonstrated. The substrate was continuously tilted about  $x$  and  $y$  axes with  $0.11^\circ$  precision, corresponding to a translation of the ion foci of 1.5 nm on the substrate. With tilting in one direction, 15 nm full width at half maximum trenches 45 nm deep were etched into a Si wafer using an  $\text{Ar}^+$  beam in a  $\text{Cl}_2$  ambient. T-shaped patterns were etched by tilting the substrates in two directions. © 2008 American Institute of Physics. [DOI: 10.1063/1.2828208]

The search for better nanopatterning methods has been the subject of intense investigations in recent years. Diblock copolymer self-assembly can produce  $\sim 20$  nm holes or lines,<sup>1-3</sup> but lacks control of pattern registration over large areas. Dip pen lithography can write complicated patterns with 15 nm linewidth using an atomic microscopy tip,<sup>4,5</sup> but patterning speed and reproducibility are not practical. Ion or electron beam proximity or projection lithography can define features finer than 20 nm,<sup>6</sup> but require fragile stencil masks with equally fine features. Imprint lithography shows promise for low-cost, high throughput fabrication, with ultimate resolution possibly in the sub-10-nm regime.<sup>7</sup> Imprint lithography is a contact process, however, and defects that could be introduced during the stamping process are a concern.<sup>8,9</sup>

Recently we reported “nanopantography” as a method for massively parallel patterning of nanosized features.<sup>10</sup> A broad, collimated, monoenergetic ion beam is directed at an array of submicron-diameter electrostatic lenses fabricated on the conductive substrate (e.g., doped Si wafer). By applying appropriate voltages to the lens electrodes, the “beamlets” entering the lenses are focused to spots that can be  $100\times$  smaller than the diameters of the lenses.<sup>10</sup> Each lens writes identical nanofeatures on the substrate, therefore, nanopantography is a *parallel* process, very different from focused electron beam or ion beam writing. Because the lens arrays are part of the substrate, the method is immune to misalignment caused by vibrations or thermal expansion. In our previous work with an  $\text{Ar}^+$  beam in the presence of  $\text{Cl}_2$  gas,  $\sim 10$  nm diam, 100 nm deep holes were etched in Si.<sup>10</sup>

When the substrate was tilted with respect to the ion beam axis, the focal points of the off-normal ion beamlets were displaced from the centers of the lens bottoms. Here, we demonstrate writing of etched nanopatterns in Si by continuously tilting the substrate.

In our previous work, we demonstrated etching of single holes,<sup>10</sup> extraction of a monoenergetic ion beam which is critical to nanopantography,<sup>11</sup> and characterization of a Ni containing plasma used for nanopantographic deposition.<sup>12</sup> The present work demonstrates a technique capable of writing *any arbitrary shapes or patterns* in a massively parallel manner. Multiple patterns that repeat with some periodicity may also be written. This can be done by further patterning the top metal layer, such that only the desired holes are addressed. Etching will occur only in the holes for which a voltage is applied to the top metal layer so that the ion beamlets are focused. The rest of the holes will have no voltage applied to the top metal layer, the beamlets will not be focused, and the current density will be too small to cause any appreciable etching.

The experimental system consists of a plasma source, ion “drift” region, wafer processing chamber, motorized stage, and load-lock chamber (Fig. 1). The motorized stage allows two-dimensional tilting of the sample, thus, enabling writing of nanopatterns. The plasma source chamber is the same as in previous reports,<sup>11,12</sup> except for a finer ( $40\ \mu\text{m}$  hole size) and more transparent (60% open area) ion extraction grid, made from woven Ni wire. The aperture underneath the grid was 11.4 mm. The drift tube was shortened from 700 to 400 mm, with two differential pumping stages, and three 600/s turbomolecular pumps to reduce charge exchange and increase ion current. The processing chamber was evacuated with a 240/s cryopump. A  $\text{Cl}_2$  nozzle was

<sup>a)</sup>Electronic mail: economou@uh.edu.

<sup>b)</sup>Electronic mail: vmdonnelly@uh.edu.

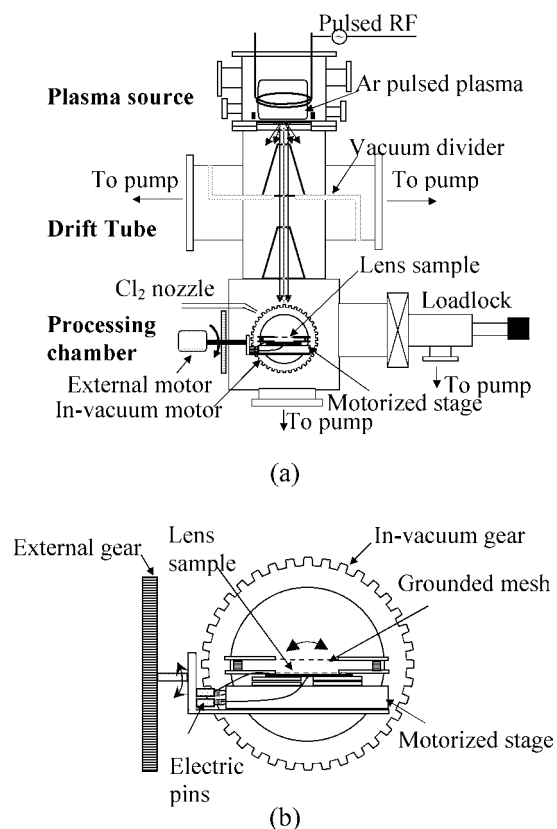


FIG. 1. (a) Schematic of nanopantography apparatus. (b) Expanded view of motorized stage.

directed at the sample, at a distance of 4 cm from the sample at the center of the processing chamber. With a plasma reactor pressure of 8 mTorr Ar, the pressures were  $1 \times 10^{-4}$ ,  $4 \times 10^{-5}$ , and  $2 \times 10^{-5}$  Torr in the first and second differentially pumped chambers, and the processing chamber, respectively. At these low pressures, the probability of charge-exchange collisions of  $\text{Ar}^+$  was less than 10% in each chamber.

The sample stage angles about the  $x$ - and  $y$ -orthogonal axes were controlled by two precision stepping motors; one outside the chamber and one in vacuum (Fig. 1). As the sample was tilted, ion focal points were translated along the bottoms of the lenses. A LABVIEW™ program controlled the movement of the stages. The minimum angular step of  $0.11^\circ$  corresponds to  $\sim 1.5$  nm translation of the ion focal point at the bottom of a 250 nm diam lens. This translation factor was determined by measuring the distance between two holes that were etched at two tilting angles. Samples were mounted on a holder and electrical connections to the top metal and substrate were made. The holder was then placed in a load-lock chamber, transferred under vacuum to the processing chamber, and plugged into a docking station (Transfer Engineering and Manufacturing, Inc., Fremont, CA) on the manipulator, containing mating electrical sockets for pins on the sample holder [Fig. 1(b)].

As with any ion-focusing electrostatic lens, to achieve the sharpest focus, one must minimize the energy spread of the extracted ion beam.<sup>13,14</sup> Previously, an ion extraction method was described for obtaining a nearly monoenergetic  $\text{Ar}^+$  beam from a capacitively coupled pulsed Ar plasma.<sup>11</sup> The plasma was pulsed on and off with a frequency of 5 kHz and a 50% duty cycle. During the power-off periods, a posi-

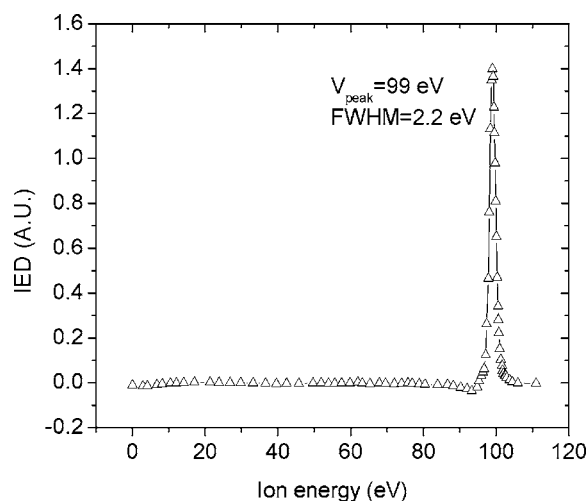


FIG. 2. Ion energy distribution of an  $\text{Ar}^+$  beam extracted from the inductively coupled pulsed plasma. The voltage pulse on the acceleration ring electrode was +100 V from 12 to 96  $\mu\text{s}$  in the afterglow. 8 mTorr pressure, 5 kHz modulation frequency, 50% duty cycle, and 100 W average plasma power.

tive dc voltage pulse was applied to an acceleration ring electrode immersed in the plasma. The plasma potential quickly attained this dc voltage and ion energy (the potential difference between this voltage and the grounded extraction grid) was thus, precisely established. In addition, the electron temperature decayed rapidly in the power-off periods, resulting in uniform plasma potential and minimal ion energy and angular spread. This same strategy was adapted to the inductively coupled pulsed plasma source used in the present system. The ion energy distribution (IED) of the extracted ion beam was measured by a gridded energy analyzer. With a +100 V on the acceleration electrode, pulsed from 12 to 96  $\mu\text{s}$  in the plasma-off period, the IED peaked at 99 eV with a measured full width at half maximum (FWHM) of 2.2 eV (Fig. 2). The actual energy spread is likely even narrower since the measured width is near the energy resolution of the analyzer ( $\sim 1\% - 2\%$ ). The current density of the ion beam delivered to the sample was  $\sim 1 \mu\text{A}/\text{cm}^2$ , an enhancement of about a factor of 15, compared to the previous system.<sup>10</sup>

The lens arrays (supplied by SEMATECH, Inc.) consisted of a 150-nm-thick Al layer on a 1000-nm-thick thermal  $\text{SiO}_2$  on a heavily-doped Si substrate. Each sample contained 200, 250, 300, 350, and 650 nm diameter lens openings. The substrate was at ground potential and the optimal ion-focusing voltage on the top electrode was obtained by ion trajectory simulations and through experiments. An  $\text{Ar}^+$  beam with ion energy of 100 eV and an effusive  $\text{Cl}_2$  beam with a  $\text{Cl}_2/\text{Ar}^+$  flux ratio of  $\sim 100:1$  were employed. The etch rate of Si is 1.3 Si atoms per  $\text{Ar}^+$  under these conditions.<sup>15</sup> In contrast, the sputtering rate without  $\text{Cl}_2$  is much slower (0.1 Si atoms per  $\text{Ar}^+$  at  $E_i = 100$  eV),<sup>16</sup> and  $\text{Cl}_2$  gas does not react with Si at room temperature.<sup>17</sup> Therefore, etching only occurs at the ion focal spots. A grounded mesh [shown in Fig. 1(b)] with 40  $\mu\text{m}$  diam holes was mounted 1.5 cm above the sample to eliminate transverse electric fields above the lenses. After etching, samples were examined by scanning electron microscopy (SEM).

Continuous V-shaped nanotrenches were written into Si by tilting a lens array in one direction from  $-5^\circ$  to  $+5^\circ$  with

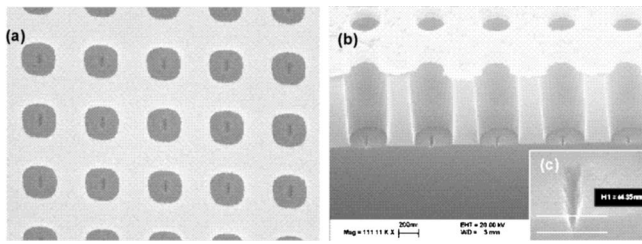


FIG. 3. Etching of nanotrenches by nanopantography: (a) top view of a portion of a 650 nm diam lens array, (b) 45° view of a portion of a cleaved 250 nm diam lens array, and (c) 45° view of an etched trench in a 250 nm diam lens.

respect to the substrate normal, in steps of  $0.5^\circ$ , using a dwell time of 10 min at each angle. Figure 3(a) is a top-down SEM image of a small portion of an array of 650 nm diam lenses, showing 200 nm long trenches etched across the center of each lens bottom. Figures 3(b) and 3(c) show a cleaved edge of a portion of 250 nm diam lenses. Each lens produced a nanotrench 150 nm long and 45 nm deep, and widths of  $\sim 30$  nm at the top and  $\sim 15$  nm FWHM. The feature sidewall is straight and somewhat tapered, with an angle of  $18^\circ$  with respect to the surface normal. The line width did not vary along the length of the trench, indicating that the degree of ion focus does not depend on the tilt angle. Similarly, T-shaped features with top linewidth of  $\sim 50$  nm in 650 nm diam lenses (Fig. 4) were etched into Si, using a step size of  $0.25^\circ$  tilted about both  $x$  and  $y$  axes and a shorter dwell time (2.5 min) at each point.

The 15 nm FWHM resolution is close to the  $\sim 16$  nm displacement expected for an ion that impinges on the lens

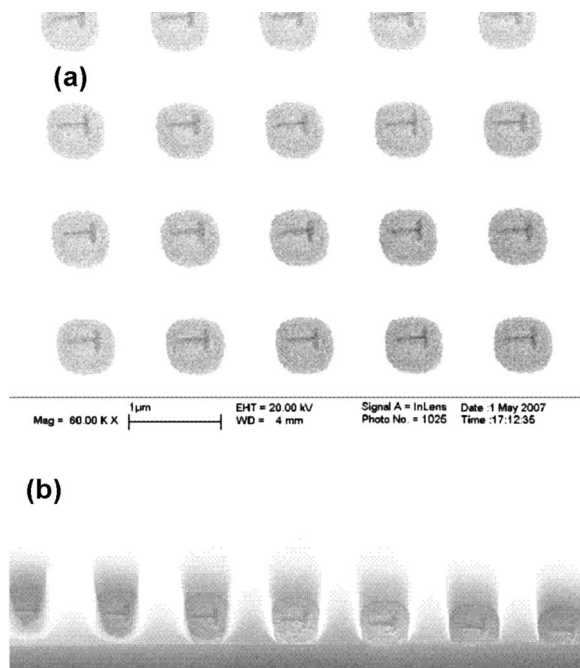


FIG. 4. Etching of T-shaped features by nanopantography: (a) top view of a portion of a 650 nm diam lens array and (b) 45° view of a portion of a 650 nm diam lens array.

array with an angle of  $0.8^\circ$  off normal. This is the maximum angle possible from the penumbra generated by the 11.4 mm diam aperture of the extraction grid and the 400 mm distance between the extraction grid and the sample. Therefore, to realize sub-10-nm nanopatterning in the future, the acceptance angle for ions must be reduced to  $<0.5^\circ$ . Reducing the aperture size is the most straightforward way to achieve this, but will also require an increase in plasma density to maintain or hopefully increase the ion flux. Such modifications are currently underway.

In summary, we have demonstrated direct writing of massively parallel nanopatterns by nanopantography. This was achieved by impinging a narrow-energy spread ( $<2.2$  eV FWHM at 100 eV)  $\text{Ar}^+$  beam on an array of ion focusing lenses built on the substrate. A computer-controlled motorized stage could be tilted about the  $x$  and  $y$  axes with an accuracy of  $0.11^\circ$ , corresponding to translation of the focal points by 1.5 nm at the bottoms of 250 nm diam lenses on the substrate. By continuously tilting the substrate in one direction, nanotrenches 150 nm long and 45 nm deep with width of  $\sim 15$  nm FWHM were etched into Si in the presence of  $\text{Cl}_2$  gas. T-shaped features were also etched into Si by tilting the substrate about both the  $x$  and  $y$  axes.

This work was supported by the National Science Foundation (NSF-NIRT-0303790 and NSF-MRI-0521523) and the Texas Advanced Research Program.

<sup>1</sup>K. W. Guarini, C. T. Black, K. R. Milkove, and L. Sundstrom, *J. Vac. Sci. Technol. B* **19**, 2784 (2001).

<sup>2</sup>C. T. Black, K. W. Guarini, G. Breyta, M. C. Colburn, R. Ruiz, R. L. Sandstrom, E. M. Sikorski, and Y. Zhang, *J. Vac. Sci. Technol. B* **24**, 3188 (2006).

<sup>3</sup>L. Sundstrom, L. Krupp, E. Delenia, C. Rettner, M. Sabcegez, M. W. Hart, H. C. Kim, and Y. Zhang, *Appl. Phys. Lett.* **88**, 243107 (2006).

<sup>4</sup>S. Hong, J. Zhu, and C. A. Markin, *Science* **286**, 523 (1999).

<sup>5</sup>L. M. Demers, D. S. Ginger, S. J. Park, Z. Li, S. W. Chung, and C. A. Mirkin, *Science* **296**, 1836 (2002).

<sup>6</sup>R. S. Dhaliwal, W. A. Enichen, S. D. Golladay, M. S. Gordon, R. A. Kendall, J. E. Lieberman, C. Pfeiffer, D. J. Pinckney, C. F. Robinson, J. P. Rockrohr, W. Stickel, and E. V. Tressler, *IBM J. Res. Dev.* **45**, 615 (2001).

<sup>7</sup>S. Y. Chou, P. R. Krauss, and P. J. Renstrom, *J. Vac. Sci. Technol. B* **14**, 4129 (1996).

<sup>8</sup>D. J. Resnick, W. J. Dauksher, D. Mancini, K. J. Nordquist, T. C. Bailey, S. Johnson, N. Stacey, J. G. Ekerdt, C. G. Willson, S. V. Sreenivasan, and N. Schumaker, *J. Vac. Sci. Technol. B* **21**, 2624 (2003).

<sup>9</sup>T. Bailey, B. Smith, B. J. Choi, M. C. Colburn, M. Meissl, S. V. Sreenivasan, J. G. Ekerdt, and C. G. Willson, *J. Vac. Sci. Technol. B* **19**, 2806 (2001).

<sup>10</sup>L. Xu, S. C. Vemula, M. Jain, S. K. Nam, V. M. Donnelly, D. J. Economou, and P. Ruchhoeft, *Nano Lett.* **5**, 2563 (2005).

<sup>11</sup>L. Xu, D. J. Economou, V. M. Donnelly, and P. Ruchhoeft, *Appl. Phys. Lett.* **87**, 041502 (2005).

<sup>12</sup>L. Xu, N. Sadeghi, V. M. Donnelly, and D. J. Economou, *J. Appl. Phys.* **101**, 013304 (2007).

<sup>13</sup>S. Namamachi, Y. Yamakage, M. Ueda, and H. Maruno, *Rev. Sci. Instrum.* **67**, 2351 (1996).

<sup>14</sup>S. Nomura, *J. Vac. Sci. Technol. B* **17**, 82 (1999).

<sup>15</sup>M. Balooch, M. Moalem, W. E. Wang, and A. V. Hamza, *J. Vac. Sci. Technol. A* **14**, 229 (1996).

<sup>16</sup>J. P. Chang, J. C. Arnold, G. H. Zau, H. S. Shin, and H. H. Sawin, *J. Vac. Sci. Technol. A* **15**, 1853 (1997).

<sup>17</sup>Y. Teraoka and I. Nishiyama, *J. Appl. Phys.* **79**, 4397 (1996).